Available online at www.sciencedirect.com
SCIENCE DIRECT
Icarus 180 (2006) 403–411
ICARUS
www.elsevier.com/locate/icarus

Understanding the behavior of Prometheus and Pandora

Alison J. Farmer [a,b,*], Peter Goldreich [a,b]

[a] *Theoretical Astrophysics, MC 130-33, Caltech, Pasadena, CA 91125, USA*
[b] *Institute for Advanced Study, Einstein Drive, Princeton, NJ 08540, USA*

Received 20 July 2005; revised 5 October 2005

Available online 6 December 2005

Abstract

We revisit the dynamics of Prometheus and Pandora, two small moons flanking Saturn's F ring. Departures of their orbits from freely precessing ellipses result from mutual interactions via their 121:118 mean motion resonance. Motions are chaotic because the resonance is split into four overlapping components. Orbital longitudes were observed to drift away from predictions based on *Voyager* ephemerides. A sudden jump in mean motions took place close to the time at which the orbits' apses were antialigned in 2000. Numerical integrations reproduce both the longitude drifts and the jumps. The latter have been attributed to the greater strength of interactions near apse antialignment (every 6.2 yr), and it has been assumed that this drift-jump behavior will continue indefinitely. We re-examine the dynamics of the Prometheus–Pandora system by analogy with that of a nearly adiabatic, parametric pendulum. In terms of this analogy, the current value of the action of the satellite system is close to its maximum in the chaotic zone. Consequently, at present, the two separatrix crossings per precessional cycle occur close to apse antialignment. In this state libration only occurs when the potential's amplitude is nearly maximal, and the "jumps" in mean motion arise during the short intervals of libration that separate long stretches of circulation. Because chaotic systems explore the entire region of phase space available to them, we expect that at other times the Prometheus–Pandora system would be found in states of medium or low action. In a low action state it would spend most of the time in libration, and separatrix crossings would occur near apse *alignment*. We predict that transitions between these different states can happen in as little as a decade. Therefore, it is incorrect to assume that sudden changes in the orbits only happen near apse antialignment.

Keywords: Orbits; Satellites of Saturn

1. Introduction

Discovered by the *Voyager* spacecraft in 1980 and 1981, Prometheus and Pandora are two small moons of Saturn. Properties of their orbits are summarized in Table 1. A series of observations starting in 1995 found that the orbital longitude of each satellite deviated by about 20° from its value as predicted by the *Voyager* ephemeris (Bosh and Rivkin, 1996; Nicholson et al., 1996; McGhee et al., 2001). Further, each satellite's mean motion underwent an abrupt change in 2000 (French et al., 2002), seen as "kinks" in their mean longitudes. Goldreich and Rappaport (2003a) (GR03a) pinpointed chaos due to the satellites' mutual gravitational interactions as the cause of these discrepancies. The system was found to have a Lyapunov exponent $\sim 0.3\ \mathrm{yr}^{-1}$. Jumps in the mean motion were attributed to the stronger interactions that occur when the orbits' apses are antialigned. Orbital integrations in GR03a reproduce the observed gradual drifts away from the *Voyager*-based predictions. Kinks in the mean longitudes are apparent every 6.2 yr, at times of apse antialignment. Goldreich and Rappaport (2003b) (GR03b) captures the essential dynamics of the system by including only interactions due to the 121:118 mean motion resonance. More complete numerical simulations of the system, which include the influences of other saturnian satellites, have been performed by Cooper and Murray (2004); Jacobson and French (2004); and Renner et al. (2005). These confirm that the simplified dynamics in GR03b is sufficient to describe the chaotic motions of Prometheus and Pandora.

* Corresponding author. MS-51, Center for Astrophysics, 60 Garden St., Cambridge, MA 02138, USA.
E-mail address: afarmer@cfa.harvard.edu (A.J. Farmer).

0019-1035/$ – see front matter
doi:10.1016/j.icarus.2005.10.005

Table 1
Properties of Prometheus and Pandora and of their orbits (from GR03b)

Quantity	Prometheus	Pandora
Symbols	Unprimed	Primed
m/M	5.80×10^{-10}	3.43×10^{-10}
λ (°)	188.53815	82.14727
n (° s^{-1})	6.797331×10^{-3}	6.629506×10^{-3}
e	2.29×10^{-3}	4.37×10^{-3}
ϖ (°)	212.85385	68.22910
$\dot{\varpi}$ (° s^{-1})	3.1911×10^{-5}	3.0082×10^{-5}

Physical explanations for the mean motion jumps have not advanced beyond those proposed by Goldreich and Rappaport: all of the above papers cite enhanced interactions at apse antialignment as the reason for the kinks in the mean longitudes observed in 2000. They do nothing to dispel the expectation that the mean longitudes will continue to display the same drift-kink behavior indefinitely into the future. A practical consequence of this belief is that orbits fitted to Cassini data avoid times around apse antialignment and assume freely precessing ellipses between these times (Porco et al., 2005).

We show that a proper understanding of the dynamics of the Prometheus–Pandora system is more subtle than previously recognized. In doing so we exploit an analogy with the dynamics of a parametric pendulum to reinterpret numerical integrations presented in GR03b. We confirm that separatrix crossings are the cause of chaos and that their rate determines the magnitude of the Lyapunov exponent. Our focus is on the precessional phase at which separatrix crossings occur. Currently the two that take place during each 6.2 yr precessional cycle occur near apse antialignment and the kinks arise during intervals of libration separated by long stretches of circulation. More generally, separatrix crossings can occur at any precessional phase, with large changes in these phases predicted on timescales of one to two decades. When crossings take place near apse alignment, the system remains chaotic but displays qualitatively different features than at present.

This paper is arranged as follows. In Section 2 we demonstrate the similarity between the dynamics of the Prometheus–Pandora interaction and that of a parametric pendulum. We study the behavior of an adiabatic parametric pendulum in Section 3. In Section 4 we apply these findings to the Prometheus–Pandora system, and discuss both the implications and the limitations of our analogy. We conclude in Section 5.

2. Similarity of equations

GR03b showed that the chaotic motions of Prometheus and Pandora arise from their 121:118 mean motion resonance. Differential precession of the two eccentric orbits splits the resonance into four discrete components whose arguments are $\psi_q = \psi - \delta_q$, with

$$\psi \equiv 121\lambda - 118\lambda', \tag{1}$$

Table 2
Properties of the four components of the 121:118 mean motion resonance (from GR03b)

Resonance, q	Period (yr) $= -2\pi/\dot{\psi}_q$	Coefficient, C_q
1	1.078	-1.08×10^{-3}
2	1.303	6.26×10^{-3}
3	1.648	-1.21×10^{-2}
4	2.239	7.82×10^{-3}

where λ and λ' are, respectively, the mean longitudes of Prometheus and Pandora, and

$$\delta_1 \equiv 3\varpi, \qquad \delta_2 \equiv 2\varpi + \varpi', \qquad \delta_3 \equiv \varpi + 2\varpi', \qquad \delta_4 \equiv 3\varpi'. \tag{2}$$

GR03b note that because of the rapid precession caused by Saturn's oblateness, interactions between the satellites produce negligible effects on their apsidal angles and orbital eccentricities. Therefore it is adequate to only treat changes in mean motions, or equivalently in the angle ψ.

The equation of motion for ψ reads (GR03b)

$$\frac{\mathrm{d}^2\psi}{\mathrm{d}t^2} = 3\big(121n'\big)^2 \frac{m}{M}\left[1 + \frac{am'}{a'm}\right] \sum_{q=1}^{4} C_q \sin(\psi - \delta_q), \tag{3}$$

where $M = 6 \times 10^{29}$ g is the mass of Saturn, and where the values of terms in Eq. (3) are given in Tables 1 and 2.

Equation (3) can be written as

$$\frac{\mathrm{d}^2\psi}{\mathrm{d}t^2} = -\omega_0^2 A(t) \sin\big[\psi - \phi(t)\big] \tag{4}$$

at time t, where $\omega_0 \simeq 3.8$ yr^{-1} and $|A| \leqslant 1$. Defining $\Psi = \psi - \phi$ and thus transforming to the frame drifting with the potential at $\dot{\phi}$, we obtain

$$\frac{\mathrm{d}^2\Psi}{\mathrm{d}t^2} = -\omega_0^2 A(t) \sin\Psi + \ddot{\phi}. \tag{5}$$

Provided $\ddot{\phi} \ll \omega_0^2 A$, we can drop the last term, leaving

$$\frac{\mathrm{d}^2\Psi}{\mathrm{d}t^2} = -\omega_0^2 A(t) \sin\Psi, \tag{6}$$

precisely the equation of motion of a parametric pendulum. The potential in which Ψ moves is given by

$$V(\Psi, t) = -\omega_0^2 A(t) \cos\Psi. \tag{7}$$

Plots of $|V|$, ϕ, $\dot{\phi}$ and $\ddot{\phi}$ are displayed in Fig. 1.[1]

The timescale for variation of $|V(t)|$ is $2\pi/|\dot{\varpi} - \dot{\varpi}'| \approx 6.2$ yr, and the fractional variation in its amplitude is of order unity. The typical oscillation period of Ψ is $\omega \sim 2\pi/|\bar{V}|^{1/2} \sim 2$ yr, so the slowness parameter $\epsilon \sim 1 \times 2/6.2 \simeq 0.3$. Thus the Prometheus–Pandora system is only marginally adiabatic.

[1] Although $\ddot{\phi} \neq 0$, we approximate $\dot{\phi}$ to be constant at -50.7 yr^{-1} when we calculate the action for the Prometheus–Pandora system. The pendulum analogy takes us a long way toward understanding the behavior of the system. We assess its validity in Section 4.2.

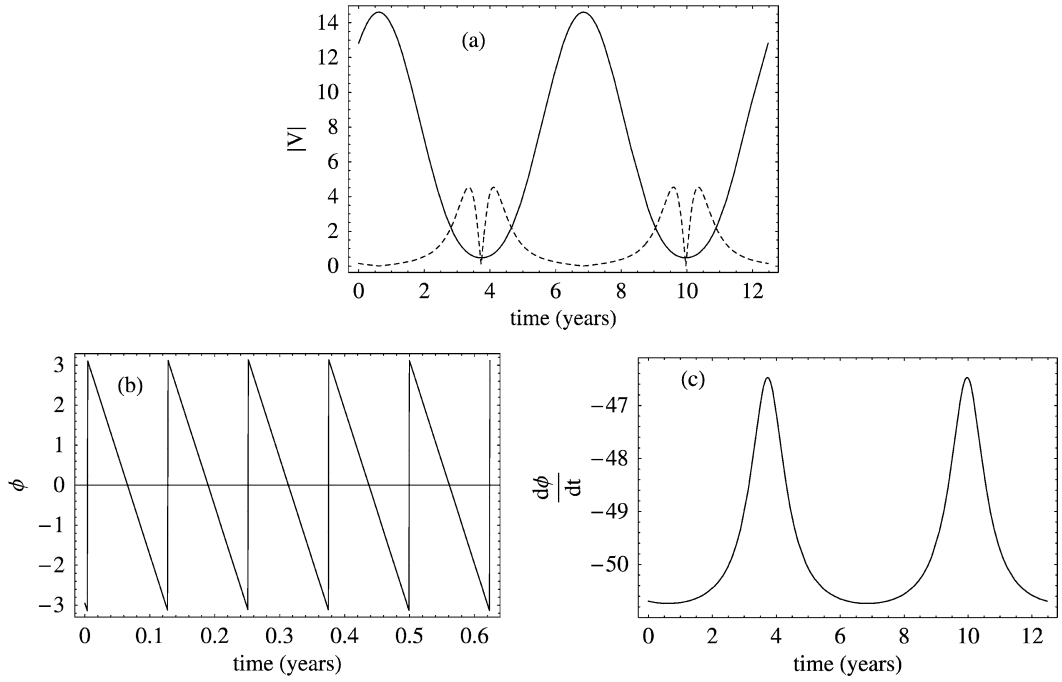

Fig. 1. Properties of the potential in which the Prometheus–Pandora system moves: (a) solid line—the amplitude of the potential as a function of time, dashed line—$\ddot{\phi}$; (b) drift phase ϕ as a function of time; (c) rate of change of the drift phase. This is the drift rate of the hills in the potential. In most of this study we ignore the variation of $\dot{\phi}$, since it is localized to a small fraction of the period.

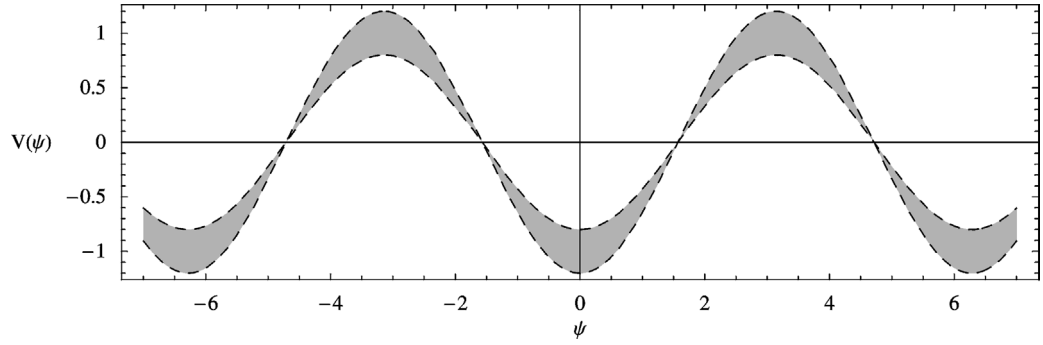

Fig. 2. The potential $V(\psi)$ in which the simplified parametric pendulum moves, for $\alpha = 0.2$. Shaded area shows range over which potential varies with time.

Rather than examine it directly, it proves instructive to consider a parametric pendulum for which adiabaticity is robust. For this we choose

$$A(t) = 1 + \alpha \cos(\kappa t), \tag{8}$$

where $\alpha < 1$ and $\kappa \ll \omega_0$, so that for small oscillations the system is adiabatic with slowness parameter

$$\epsilon \sim \alpha\kappa/\omega_0 \ll 1. \tag{9}$$

Without loss of generality we can set $\omega_0 = 1$. This potential is illustrated in Fig. 2.

2.1. Integration

All integrations in this paper are done in *Mathematica 5* using a Runge–Kutta routine with fixed step size. Care is taken to maintain numerical accuracy at a level such that differences in initial conditions determine the rates at which neighboring trajectories diverge.

3. Behavior of the simplified parametric pendulum

A simple pendulum can exhibit motion of two kinds[2]: libration for $E < |V|$ in which ψ is trapped in a valley, and circulation for $E > |V|$ in which ψ passes over the hills. Between these two regimes lies the separatrix, a singular trajectory of infinite period with energy

$$E = \dot{\psi}^2/2 - A\cos\psi = A. \tag{10}$$

As $A(t)$ varies, the motion of a parametric pendulum may switch between these two regimes. Transitions from large amplitude librations to circulations may occur as the potential shallows. Likewise, transitions in the opposite direction can take place as the potential steepens. No matter how slowly the potential varies, adiabatic invariance is violated during separatrix crossings.

[2] For a simple pendulum, A is independent of time.

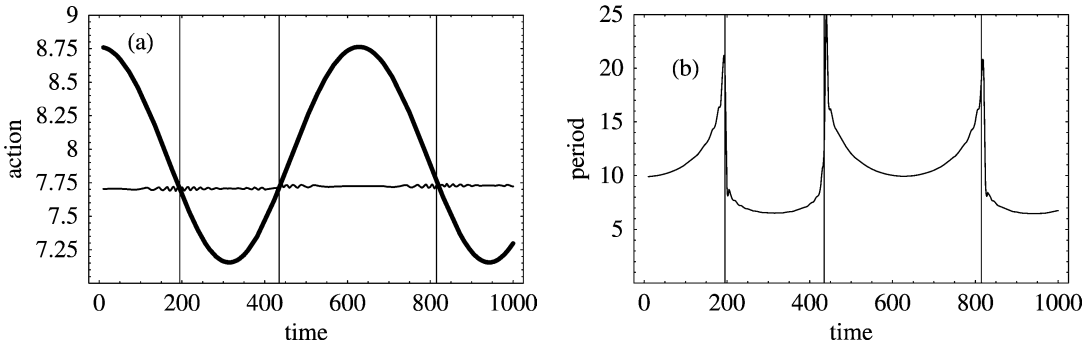

Fig. 3. For the model parametric pendulum system with $\alpha = 0.2$, $\kappa = 0.01$: (a) action as a function of time; thick line is separatrix action and thin line is system action. (b) System period as a function of time, with vertical lines at locations of separatrix crossings, where the period becomes large.

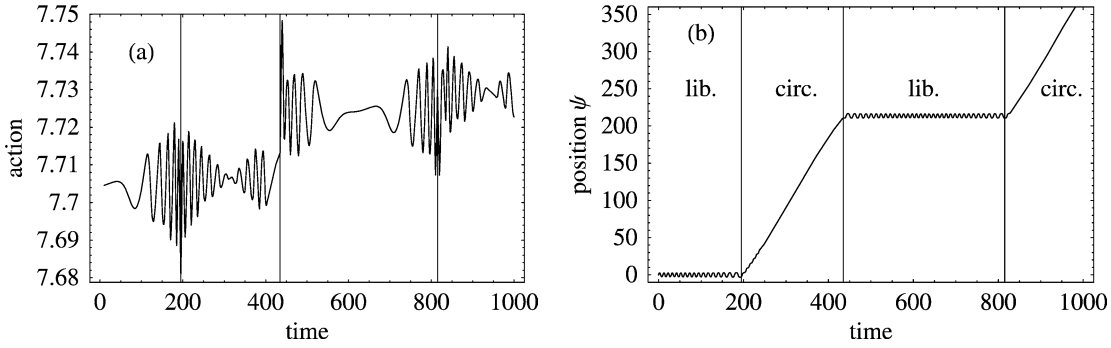

Fig. 4. For the same system as in Fig. 3: (a) zoom-in on system action, showing jumps in action at separatrix crossings (marked by vertical lines). (b) Evolution of $\psi(t)$, showing transitions from libration to circulation and vice versa at separatrix crossings.

For an adiabatic system the action, $J(t)$, remains nearly constant as $A(t)$ varies. We calculate $J(t)$ by freezing $A(t)$ and integrating over a period[3]:

$$J(t) = \oint p\,\mathrm{d}q = \oint \dot{\psi}\,\mathrm{d}\psi = \oint \sqrt{2\big[E(t) - V(\psi')\big]}\,\mathrm{d}\psi'. \quad (11)$$

In a similar manner, we obtain the period from $P(t) = \oint \mathrm{d}q/\dot{q}$. On the separatrix,

$$J_{\mathrm{sep}}(t) = 8A(t)^{1/2}. \quad (12)$$

Fig. 3 illustrates some aspects of the behavior of a parametric pendulum characterized by $\kappa = 0.01$, $\alpha = 0.2$, i.e., slowness parameter $\epsilon \sim 0.002$. We see that $J(t)$ maintains a nearly constant value as both the action on the separatrix and the period undergo large variations. Jumps in action at separatrix crossings are displayed at higher resolution in Fig. 4 along with the evolution of $\psi(t)$.

3.1. Separation in phase space and Lyapunov exponent

The rate at which neighboring trajectories in phase space separate is of practical interest because it limits our ability to make predictions about the future. For chaotic systems, small errors in initial conditions amplify exponentially, invalidating long-term predictions. To track the separation of two neighboring trajectories, we Taylor expand the equation of motion (Eq. (6)) to first order in $\Delta\psi$:

$$\frac{\mathrm{d}^2\Delta\psi}{\mathrm{d}t^2} = -A(t)\omega_0^2\Delta\psi\cos\psi. \quad (13)$$

The phase space separation,

$$S(t) = \left[\Delta\psi^2 + \left(\frac{\mathrm{d}\Delta\psi}{\mathrm{d}t}\right)^2\right]^{1/2}, \quad (14)$$

is calculated by the simultaneous integration of Eqs. (6) and (13). The Lyapunov exponent, ℓ, is the limit as $t \to \infty$ of $(\ln S)/t$. From Fig. 5 we find $\ell \simeq 0.0022$, which is close to the rate of separatrix crossings.

The Lyapunov exponent measures the average exponentiation rate of the divergence of neighboring trajectories. Fig. 5a shows how this divergence proceeds through a few separatrix crossings. At each crossing the separation S between trajectories undergoes a sudden jump, corresponding to the differential phase delay introduced there between neighboring trajectories. Between crossings $S(t)$ displays an oscillation superposed on a linear trend. The oscillation reflects the periodic motion of the pendulum, and the linear variation is due to the period difference between neighboring trajectories. Both the jumps in S at separatrix crossings and the linear variations between them produce an increase of S on average. Since on average S and its slope change by a constant fractional amount at separatrix crossings, $S(t)$ grows exponentially.

[3] When the system is in libration, we integrate over only half a period of the motion, because otherwise the action changes by a factor of 2 across the separatrix at fixed energy.

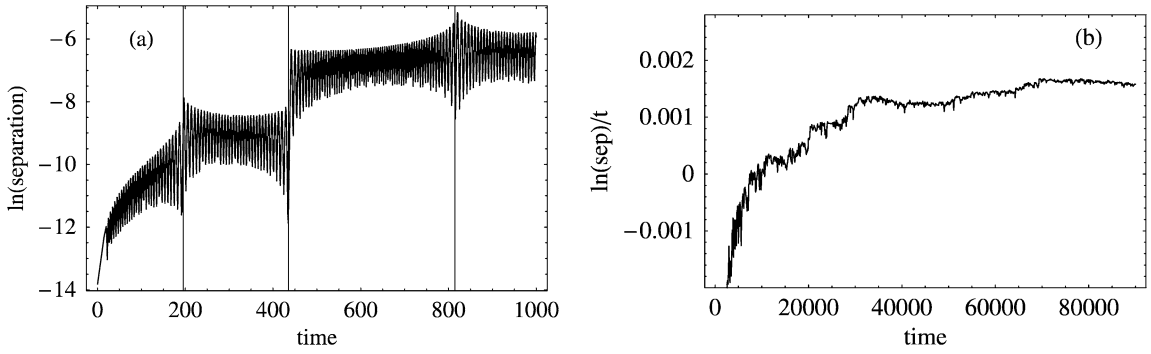

Fig. 5. For the same system as in Fig. 3, we illustrate the separation of neighboring trajectories in phase space. (a) A plot of the phase space separation as a function of time shows the jumps in both the separation and the rate of separation that occur at separatrix crossings. (b) A longer integration gives the system Lyapunov exponent ℓ as the asymptotic value of ln(separation)/time at late time, which from the plot is $\ell \sim 0.002$.

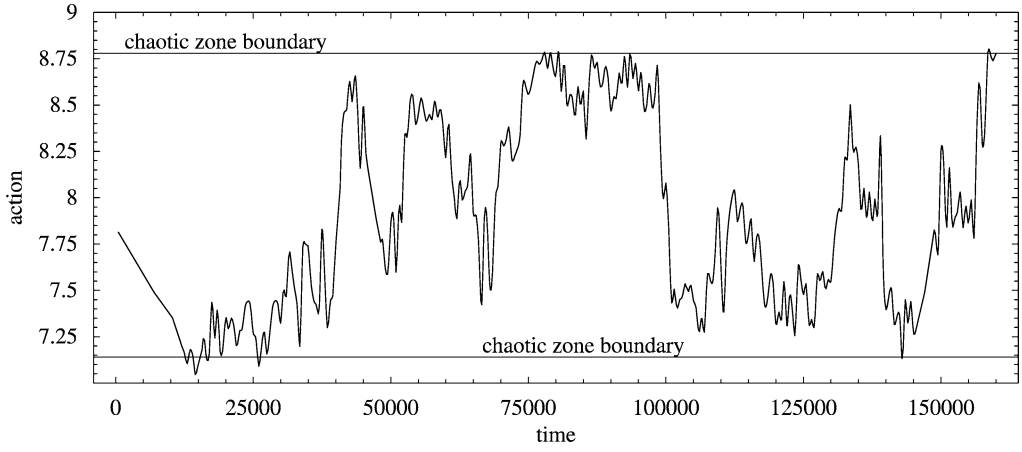

Fig. 6. Using a less adiabatic model parametric pendulum than in Fig. 3 ($\kappa = 0.1$, $\alpha = 0.2$), we plot the value of the system action over about 5000 separatrix crossings. The action diffuses more rapidly than that in Fig. 3, allowing us to more efficiently illustrate wandering across the entire chaotic zone.

3.2. *Excursions in the chaotic zone*

Only trajectories that come close to the separatrix are chaotic. The range in action over which there is chaotic behavior is

$$\Delta J_{\rm cz} \simeq 8\left(A_{\rm max}^{1/2} - A_{\rm min}^{1/2}\right) \simeq 8\alpha. \tag{15}$$

A system that starts with action outside this zone never crosses the separatrix and undergoes regular motion. A system that starts within it eventually explores the entire range of chaotic actions. Coverage of phase space is uniform in the chaotic region.

Adiabaticity is violated along trajectories that cross a separatrix and the action jumps by

$$\Delta J = -4\frac{\dot{A}}{A}\ln\left[2\cos\left(\frac{\pi}{2}\sin\frac{\psi_s}{2}\right)\right], \tag{16}$$

where ψ_s is the phase of the pendulum at which $E = E_{\rm sep}$ (Timofeev, 1978). The validity of Eq. (16) requires that $\dot{A}$ be constant while the trajectory crosses the separatrix. However, $\dot{A}$ varies on the timescale $\delta t = |\dot{A}/\ddot{A}| = |\tan\kappa t/\kappa|$ which vanishes at the extrema of A. Thus Eq. (16) does not apply within boundary layers of width δJ at the top and bottom of the chaotic zone. We estimate $\delta J \approx C\alpha\kappa^2$, where C is a (large) dimensionless number.

Fig. 6 displays the quasi-random wandering ("adiabatic chaos," Neishtadt, 1991) of the action of a model system with $\alpha = 0.2$, $\kappa = 0.1$ during approximately 5000 separatrix crossings. "Sticking" near the top and bottom of the chaotic zone is a consequence of the smaller size of the action jumps in these regions as predicted by Eq. (16); $\dot{A}/A = 0$ at the extrema of $A(t)$.

Consider the distribution of jump sizes. When crossing a separatrix, the system trajectory passes over a potential peak. Smaller margins of clearance correspond to slower passages and result in larger jumps in the action. The term $\sin(\psi_s/2)$ is proportional to the difference between the system's energy and the separatrix energy when the system makes its last passage through a potential trough prior to crossing a separatrix. We construct the probability distribution $P(\Delta J)$ of jump sizes under the assumption that $\sin(\psi_s/2)$ is uniformly distributed between ± 1. Over many separatrix crossings the action performs a quasi-random walk in which the diffusion constant is proportional to $\int {\rm d}(\Delta J) P(\Delta J)(\Delta J)^2$. From the plot of the integrand in Fig. 7, we see that jumps larger than $8\dot{A}/A$, which comprise about 4% by number, contribute about half of the diffusivity.

Integrating over jump size, we obtain a diffusion coefficient:

$$D \simeq 0.82\left(\frac{4\dot{A}}{A}\right)^2\frac{\kappa}{\pi}, \tag{17}$$

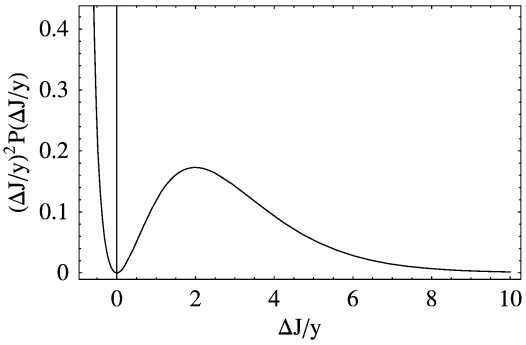

Fig. 7. The system action diffuses through the chaotic zone due to quasi-random jumps in action at separatrix crossings. The jump size is given by Eq. (16), and assuming a uniform distribution of $\sin(\psi_s/2)$, we can construct a probability distribution $P(\Delta J)$ for jump size. The contribution to the diffusivity from a given jump size ΔJ is proportional to $(\Delta J)^2 P(\Delta J)$. This quantity is plotted in the figure, normalizing jump size to $y = 4\dot{A}/A$. Jumps of more than 2 times this size contribute about half of the diffusivity while only contributing about 4% by number.

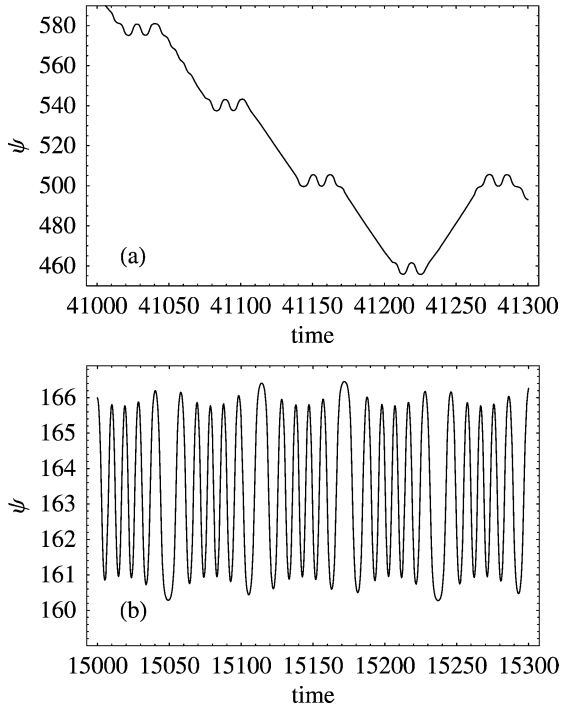

Fig. 8. Evolution of the pendulum in Fig. 6, showing the behavior of ψ when the action is close to the (a) top and (b) bottom of the chaotic zone.

where π/κ is the mean time between separatrix crossings. Taking values appropriate to the center of the chaotic zone, we estimate the zone crossing time

$$t_c \sim \frac{J_{cz}^2}{D} \sim 15{,}000, \tag{18}$$

in reasonable agreement with that observed in Fig. 6.

The pendulum mostly librates or mostly circulates, according to whether its action is close to the minimum or maximum value in the chaotic zone. This is illustrated in Fig. 8. As expected, the system samples each type of behavior.

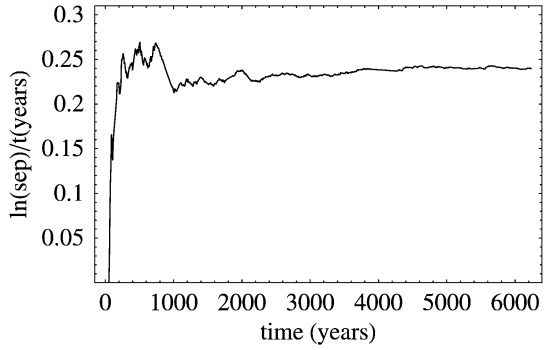

Fig. 9. Determination of the Lyapunov exponent for the Prometheus–Pandora system: this plot is analogous to Fig. 5b for the model parametric pendulum, in which the Lyapunov exponent is given by the late-time value of ln(separation)/time.

4. Prometheus and Pandora

Now we return to the Prometheus–Pandora system and detail similarities between its behavior and that of a parametric pendulum. Although our interpretation of the satellites' motions rests on the pendulum analogy, we integrate the full equation of motion (Eq. (5)) for $\psi(t)$ and the linear equation for the tangent vector $\Delta\psi(t)$ derived from it. Because the system is chaotic, it explores the entire accessible region of phase space for arbitrary initial data. We find it most convenient to adopt the initial data used by GR03b for easier comparison between their results and ours. A long integration yields a Lyapunov exponent $\ell \sim 0.3\ \mathrm{yr}^{-1}$, in agreement with that found by GR and other authors (see Fig. 9).

The variations of J and ψ for the satellite system (plotted in Fig. 10) are reminiscent of those of the analogous variables pertaining to the parametric pendulum as illustrated in Fig. 4. Similar patterns of switching between libration and circulation are exhibited by each system. Fractional variations of the action are larger in the satellite system because of its lower adiabaticity.

4.1. Where separatrix crossings occur

GR03ab and subsequent authors state that jumps in the mean motions occur near apse antialignment. Apse antialignment corresponds to the time of maximum amplitude of the potential. We see in Fig. 10 that separatrix crossings currently occur in that region. A similar behavior is seen in Fig. 8a, in which the action is close to its maximum value in the chaotic zone. Jumps in mean motion correspond to intervals spent in libration amidst stretches of circulation during which ψ increases monotonically. Changes in the slope, $\dot{\psi}$, from one episode of circulation to the next reflect changes in the action at the intervening separatrix crossings. The jumps are not *due* to chaos; rather they are due to the separatrix crossings, which *also* give rise to chaos. Changes in the circulation rate can be predicted, but only with an error that increases at every separatrix crossing.

A chaotic system explores the entire chaotic zone in phase space. We expect the Prometheus–Pandora system to sample states that are unlike its current state in which the separatrix

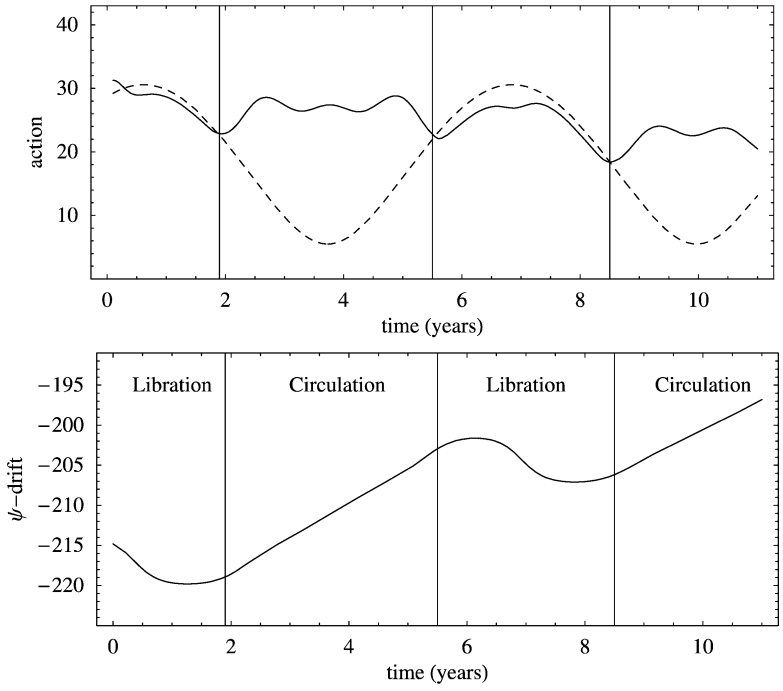

Fig. 10. Action and ψ for the Prometheus–Pandora system for the first 12 yr of integration, showing changes in the regime of motion at separatrix crossings, as indicated by vertical lines. The dashed line denotes the separatrix action. The unit of action for the Prometheus–Pandora system is $\mathrm{rad}^2\,\mathrm{yr}^{-1}$ throughout.

crossings occur near apse antialignment as seen in Fig. 8a. Averaged over time, separatrix crossings should not be restricted to a narrow range of precessional phase. In particular, states in which the separatrix crossings take place near apse alignment, such as shown in Fig. 8b, must also be sampled. Results from our integrations displayed in Fig. 11 confirm this expectation; the system experiences both states in which it is mostly in circulation and those in which it is mostly in libration. Separatrix crossings, accompanied by sudden changes in the behavior of $\psi(t)$, happen at all precessional cycles. Switching between regimes of behavior does not require a "kick" as such; the requirement is that the potential change so that the system action moves to the other side of the separatrix action. This can happen as easily near apse alignment as near apse antialignment.

A long integration confirms that the action wanders throughout the chaotic zone (Fig. 12, cf. also Fig. 6). Eqs. (17) and (18) predict that it takes ∼170 yr for the action to diffuse all the way across the zone. Due to the weak adiabaticity in this case, a single large jump can span a large fraction of the total range of action. Flipping between moderately high and moderately low action states can therefore occur in a much shorter time, as seen in Fig. 12.

Within measurement errors, a variety of orbits fit the best orbital data for Prometheus and Pandora. Renner et al. (2005) find that after two separatrix crossings (their 2004 point), there is an uncertainty of 0.2° in the longitude of each satellite.[4] Starting from this level of positional uncertainty and holding all other orbital elements fixed, we integrate forward in time a set of 3 trajectories spanning the error range. The results are shown in Fig. 13, in which the action for each trajectory is plotted against the separatrix action. In only 15 yr from the start of our integration, one of the trajectories has already transitioned from a state of high to low action (due to experiencing a large jump). This illustrates that only a small uncertainty in positions can rapidly amplify to give a qualitative change in system behavior.

4.2. Limitations of the analogy

The Prometheus–Pandora system is not strongly adiabatic, since only about 3 periods of oscillation take place during the modulation of the potential. Because the amplitude of the potential varies substantially over the period of motion, we expect our frozen potential assumption to lead to uncertainties of order half a period of the motion in the positioning of the separatrix crossings. However, we have seen that the crossing positions are adequately located by this method.

A more serious problem is the fact that we do not fulfill the condition $\ddot{\phi} \ll |V(t)|$ throughout all of the precessional cycle. The dashed line plotted in Fig. 1 shows the magnitude of the $\ddot{\phi}$ term in comparison with $|V(t)| = |\partial V/\partial\psi|$. For about one third of the time (around apse alignment), we do not fulfill this condition, and the pendulum equation does not describe the system well at all. During these times, the system is essentially governed by $\ddot{\Psi} \simeq -\ddot{\phi}$, so Ψ appears to circulate. Perhaps then we cannot define a separatrix crossing near apse alignment. We do find some evidence (not detailed in this paper) that greater jumps in the separation of trajectories occur near apse antialignment than near apse alignment. Undeniably however, changes in the evolution of $\psi(t)$ occur throughout the precessional cycle (Fig. 11), and this statement is independent of the pendulum analogy, since it is based on integrations of the full equation

[4] This is about the same as the size of a single *HST* error box at Saturn.

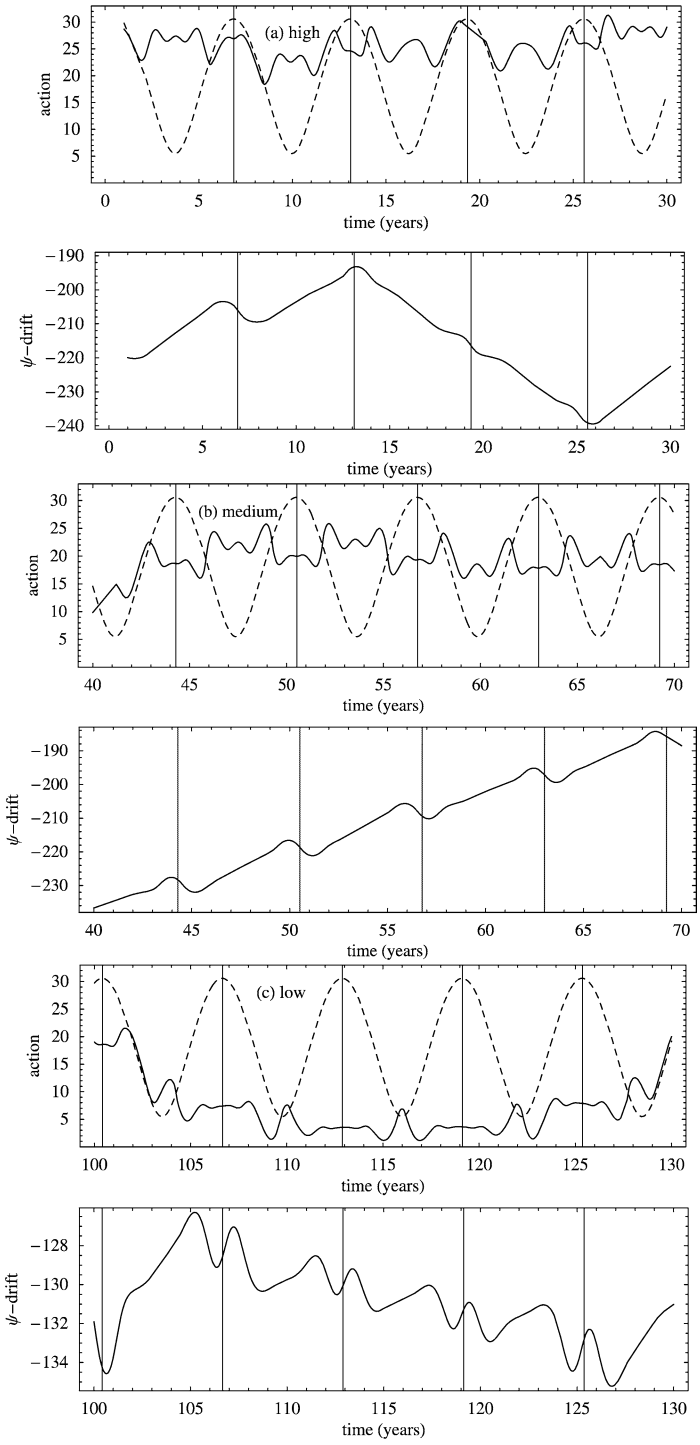

Fig. 11. Examples of high, medium, and low action states for the Prometheus–Pandora system. Vertical lines indicate times of apse antialignment, *not* separatrix crossings, which themselves occur at different precessional phases in these three cases. Dashed lines are separatrix action.

of motion, Eq. (5). The behavior of the orbits between apse antialignments certainly cannot always be fitted using freely precessing ellipses.

5. Summary and conclusions

The equations of motion of the Prometheus–Pandora resonant system are well represented by those of a parametric pendulum. Despite the low degree of adiabaticity of the system, the same regimes of behavior exist as found in a more adiabatic model system. Using this analogy, we have explained the nature of the "kinks" in mean longitude seen in both observations and simulations as short episodes of libration between long stretches of circulation. We caution that the system will not continue indefinitely to display periods of drift with intervening kinks: in as little as 15 yr, the evolution of the mean motions could be drastically different. Sudden changes in be-

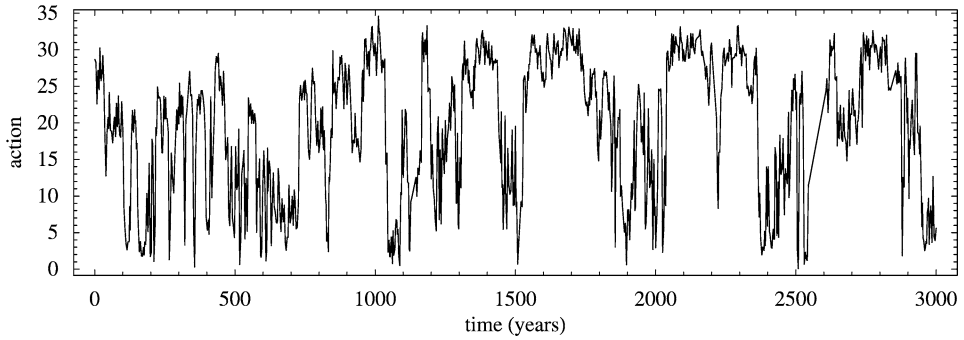

Fig. 12. Wandering of the action of the Prometheus–Pandora system: analogous to Fig. 6 for a model pendulum, this clearly delineates the chaotic zone.

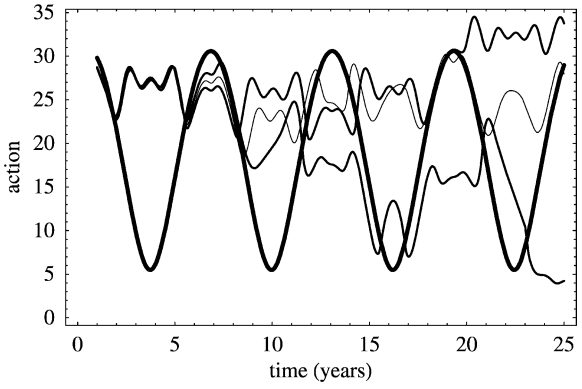

Fig. 13. We start with three sets of initial conditions of Prometheus and Pandora corresponding to 0.2° uncertainty in the longitude of each satellite, and plot the action (along with the separatrix action, thick line) for each of these trajectories. In as little as 15 yr, one of these trajectories has transitioned from a high to a low action state.

havior (and increased uncertainties in predictions) can happen far from times of apse antialignment.

Acknowledgments

This research was supported by NASA Grant PGG 344-30-55-07 and NSF Grant AST 00-98301. A.J.F. thanks the Institute for Advanced Study for its hospitality.

References

Bosh, A.S., Rivkin, A.S., 1996. Observations of Saturn's inner satellites during the May 1995 ring-plane crossing. Science 272, 518–521.

Cooper, N.J., Murray, C.D., 2004. Dynamical influences on the orbits of Prometheus and Pandora. Astron. J. 127, 1204–1217.

French, R.G., McGhee, C.A., Dones, L., Lissauer, J.J., 2002. Saturn's wayward shepherds: The perigrinations of Prometheus and Pandora. Icarus 62, 144–171.

Goldreich, P., Rappaport, N., 2003a. Chaotic motions of Prometheus and Pandora. Icarus 162, 391–399. GR03a.

Goldreich, P., Rappaport, N., 2003b. Origin of chaos in the Prometheus–Pandora system. Icarus 166, 320–327. GR03b.

Jacobson, R.A., French, R.G., 2004. Orbits and masses of Saturn's coorbital and F-ring shepherding satellites. Icarus 172, 382–387.

McGhee, C.A., Nicholson, P.D., French, R.G., Hall, K.J., 2001. HST observations of saturnian satellites during the 1995 ring plane crossings. Icarus 152, 282–315.

Neishtadt, A.I., 1991. Probability phenomena due to separatrix crossing. Chaos 1, 42–48.

Nicholson, P.D., Showalter, M.R., Dones, L., French, R.G., Larson, S.M., Lissauer, J.J., McGhee, C.A., Seitzer, P., Sicardy, B., Danielson, G.E., 1996. Observations of Saturn's ring-plane crossings in August and November 1995. Science 272, 509–515.

Porco, C.C., and 34 coauthors, 2005. Cassini imaging science: Initial results on Saturn's rings and small satellites. Science 307, 1226–1236.

Renner, S., Sicardy, B., French, R.G., 2005. Prometheus and Pandora: Masses and orbital positions during the Cassini tour. Icarus 174, 230–240.

Timofeev, A.V., 1978. On the constancy of the adiabatic invariant when the nature of the motion changes. JETP 48, 656–659.